Onset of convection in a porous layer with continuous periodic horizontal stratification. Part II. Three-dimensional convection

D. A. S. Rees[a] ; A. Barletta[b*]

[a] *Department of Mechanical Engineering, University of Bath,*

Claverton Down, Bath BA2 7AY, U.K.

[b] *Department of Industrial Engineering, Alma Mater Studiorum Università di Bologna,*

Viale Risorgimento 2, Bologna 40136, Italy

D.A.S.Rees@bath.ac.uk

antonio.barletta@unibo.it

Abstract

The onset of convection in a porous layer which is heated from below is considered. In particular we seek to determine the effect of spatially periodic variations in the permeability field on the identity of the onset mode as a function of both the period P of this variation and its amplitude A. A Floquet theory is assumed in order to ensure that the analysis is as general as possible. It is found that convection is always three dimensional and that the critical Rayleigh number always decreases as either the period or the amplitude of the permeability variation increases. Furthermore, the corresponding Floquet exponent ν is either zero or 1, and the range of values of P over which $\nu = 1$ corresponds to the favoured mode has been obtained as a function of A.

Key words: *Porous medium; Linear stability; Horizontal layer; Heterogeneity; Nonuniform permeability; Floquet theory*

*Corresponding author

1 Introduction

The onset of convective instability in a porous layer with a vertical temperature gradient has been the subject of very considerable attention particularly in the course of the last few decades. The first studies on this topic [1, 2] were formulations of the classical Rayleigh-Bénard problem within the context of filtration processes in porous media as modelled through Darcy's law [3]. A development of these early studies on what might be called the Darcy-Bénard problem, was carried out by Palm et al. [4] in order to investigate the nonlinear effects under slightly supercritical conditions. These authors obtained an expression for the Nusselt number to high order in the supercritical parameter $(Ra - Ra_c)/Ra$, where Ra is the Rayleigh number and $Ra_c = 4\pi^2$ is its critical value at the onset of instability [3].

While there are many different extensions that one might apply to the Darcy-Bénard problems, some of which are the adoption of Brinkman and/or inertia effects, the dropping of the assumption of local thermal nonequilibrium, and the consideration of inclined layers or ones which conducting boundaries, the one which we concentrate on here is the effect of a heterogeneous permeability field. Heterogeneity could comprise layered materials or media where the permeability varies continuously with one or more coordinates, or else it could be random. McKibbin and O'Sullivan [5] studied a horizontally layered material and showed that large permeability differences are required for the multilayered medium to display onset conditions different from those for a homogeneous layer. This analysis was developed further by Rees and Riley [6] by taking into account weakly nonlinear effects and they showed that double or multiple minimum loci for the Rayleigh number may exist at onset of instability. Studies of the Darcy-Bénard problem for heterogeneous porous media were carried out also by Nield and Simmons [7].

A situation where the permeability undergoes a periodic change was envisaged by De Wit and Homsy [8, 9]. However, the kind of instability investigated by these authors is definitely different from the buoyancy-induced Rayleigh-Bénard instability. On the other hand, the physical effect leading to the instability is a concentration-dependent viscosity in the binary fluid saturating the porous medium. Much more closely related to the present paper is the work of Rees and Tyvand [10] (hereinafter referred to as Part 1) who considered a porous layer with a permeability which varies periodically in a horizontal direction. The analysis carried out in that paper was two-dimensional thus limiting the study to the behaviour of transverse rolls, i.e. ones with axes that are perpendicular to the direction of the x-axis where the permeability changes periodically.

The aim of this contribution is to extend the investigation reported by Rees and Tyvand [10] from two-dimensional to three-dimensional modes. The Floquet theory which was employed by Rees and Tyvand [10] to determine the selected two-dimensional modes of instability employed in order to determine whether two dimensional modes or three dimensional modes form the favoured

onset mode.

2 Governing equations

We consider a plane porous layer saturated by a Newtonian fluid. The thickness of the layer is H. The boundary planes at $z = 0$ and $z = H$ are impermeable and isothermal, and are held at the temperatures T_h and T_c, respectively, where $T_h > T_c$. The permeability, K, varies periodically in the x-direction and it satifies the following trigonometrical law,

$$K = K_0 \left[1 + A\cos(\lambda x/H)\right], \tag{1}$$

where K_0 is the mean permeability, $A \in [0, 1)$ is a dimensionless amplitude, and λ is a dimensionless wavenumber which is such that $2\pi H/\lambda$ is the period of the permeability distribution.

The onset of convection in the porous layer is carried out under the following assumptions: (i) Darcy's law holds; (ii) the Oberbeck-Boussinesq approximation may be applied; (iii) the effective thermal conductivity and the effective volumetric heat capacity (the average product of the density and the specific heat) of the saturated porous medium are approximately uniform; (iv) there is local thermal equilibrium between the solid phase and the fluid phase; (v) no internal heating effect occurs. We can express the governing equations in a dimensionless form by adopting the scalings,

$$\begin{aligned} &\frac{1}{H}\,(x, y, z) \to (x, y, z)\,, \quad \frac{\alpha_m}{\sigma H^2}\,t \to t, \quad \frac{H}{\alpha_m}\,(u, v, w) \to (u, v, w)\,, \\ &\frac{T - T_c}{T_h - T_c} \to T, \quad \frac{K_0}{\mu\alpha_m}\,p \to p. \end{aligned} \tag{2}$$

Here, x, y, z and t denote the Cartesian coordinates and time, u, v, w are the velocity components, T is the temperature, p is the dynamic pressure, α_m is the effective thermal diffusivity of the saturated porous medium, μ is the fluid viscosity, and σ is the ratio between the effective volumetric heat capacity of the saturated porous medium and the volumetric heat capacity (the product of the density and the specific heat) of the fluid.

On account of Eq. (2), the dimensionless local balance equations for mass, momentum and heat transport may be written as

$$\frac{\partial u}{\partial x} + \frac{\partial v}{\partial y} + \frac{\partial w}{\partial z} = 0, \tag{3a}$$

$$u = -F(x)\,\frac{\partial p}{\partial x}, \quad v = -F(x)\,\frac{\partial p}{\partial y}, \quad w = -F(x)\left(\frac{\partial p}{\partial z} - Ra\,T\right), \tag{3b}$$

$$\nabla^2 T = \frac{\partial T}{\partial t} + u\,\frac{\partial T}{\partial x} + v\,\frac{\partial T}{\partial y} + w\,\frac{\partial T}{\partial z}, \tag{3c}$$

while the boundary conditions are expressed as

$$\begin{aligned} &z = 0: \qquad w = 0, \quad T = 1, \quad \frac{\partial p}{\partial z} = Ra, \\ &z = 1: \qquad w = 0, \quad T = 0, \quad \frac{\partial p}{\partial z} = 0. \end{aligned} \tag{4}$$

Here, $F(x)$ and the Darcy-Rayleigh number Ra are defined respectively as,

$$F(x) = 1 + A\cos(\lambda x), \quad Ra = \frac{\rho_c g \beta \left(T_h - T_c\right) K_0 H}{\mu \alpha_m}, \tag{5}$$

where ρ_c is the fluid density at the reference temperature T_c, g is the modulus of the gravitational acceleration $\mathbf{g}$, and β is the thermal expansion coefficient of the fluid.

The aim of this paper is to understand how the onset of three dimensional convection depends on the values of the nondimesnional parameters, A, P and ν, where A is the amplitude of the permeability variation, $P = 2\pi/\lambda$ is the period of that variation, and ν is the Floquet exponent to be introduced below.

3 Basic solution and analysis of linear disturbances

A basic state which is a stationary solution of Eqs. (3) and (4) with a zero velocity exists and is given by

$$u_b = v_b = w_b = 0, \quad T_b = 1 - z, \quad p_b = Ra\, z \left(1 - \frac{z}{2}\right), \tag{6}$$

where the subscript b denotes the "basic solution". We introduce small-amplitude disturbances of the basic solution, Eq. (6), as follows,

$$(u, v, w) = (u_b, v_b, w_b) + \varepsilon \left(U, V, W\right), \quad T = T_b + \varepsilon\theta, \quad p = p_b + \varepsilon P, \tag{7}$$

where ε is a perturbation parameter, such that $|\varepsilon| \ll 1$. We now substitute Eq. (6) and Eq. (7) into Eqs. (3) and (4), and neglect terms which are of $O(\varepsilon^2)$. Thus, the system of linearised disturbance equations is given by

$$\frac{\partial U}{\partial x} + \frac{\partial V}{\partial y} + \frac{\partial W}{\partial z} = 0, \tag{8a}$$

$$U = -F(x)\,\frac{\partial P}{\partial x}, \quad V = -F(x)\,\frac{\partial P}{\partial y}, \quad W = -F(x)\left(\frac{\partial P}{\partial z} - Ra\,\theta\right), \tag{8b}$$

$$\nabla^2\theta = \frac{\partial \theta}{\partial t} - W, \tag{8c}$$

$$z = 0, 1: \qquad W = 0, \quad \theta = 0. \tag{8d}$$

A pressure-temperature formulation is obtained by substituting Eq. (8b) into Eq. (8a), so that we finally obtain

$$\nabla^2 P = Ra\,\frac{\partial \theta}{\partial z} - G(x)\,\frac{\partial P}{\partial x}, \tag{9a}$$

$$\nabla^2\theta = \frac{\partial \theta}{\partial t} + F(x)\left(\frac{\partial P}{\partial z} - Ra\,\theta\right), \tag{9b}$$

$$z = 0, 1: \qquad \frac{\partial P}{\partial z} = 0, \quad \theta = 0, \tag{9c}$$

where

$$G(x) = \frac{F'(x)}{F(x)} = -\frac{A\lambda \sin(\lambda x)}{1 + A\cos(\lambda x)}, \tag{10}$$

and where the prime denotes an ordinary derivative with respect to x.

Equations (9) may be solved as an eigenvalue problem which defines the marginal stability condition for the Darcy-Rayleigh number Ra. However, there is a natural periodicity in the x-direction which is caused by the permeability variations, and this is not necessarily one which will yield the smallest value of the critical Rayleigh number. Therefore we may use Floquet theory to attempt to maximise the range of available disturbances that may be considered. Therefore we may write P and θ as

$$P(x, y, z, t) = \mathfrak{Re}\{Ra\, f(x) e^{i(ky + \lambda\nu x/2 - \omega t)}\} \cos(\pi z), \tag{11a}$$

$$\theta(x, y, z, t) = \mathfrak{Re}\{h(x) e^{i(ky + \lambda\nu x/2 - \omega t)}\} \sin(\pi z), \tag{11b}$$

where k is the wave number, ω is a temporal frequency and ν is the Floquet exponent. All three of these parameters are real provided that marginal stability is considered. Substitution of Eq. (11) into Eqs. (9) yields

$$\left(f'' + i\lambda\nu f' - \tfrac{1}{4}\lambda^2\nu^2 f\right) + G(x)\left(f' + \tfrac{1}{2}i\lambda\nu f\right) - \left(k^2 + \pi^2\right) f - \pi h = 0, \tag{12a}$$

$$\left(h'' + i\lambda\nu h' - \tfrac{1}{4}\lambda^2\nu^2 h\right) - \left[k^2 + \pi^2 - i\omega\right] h + Ra\, F(x)\,(h + \pi f) = 0. \tag{12b}$$

These equations are then solved subject to the periodicity conditions,

$$f(0) = f(P), \quad f'(0) = f'(P), \quad h(0) = h(P), \quad h'(0) = h'(P), \tag{13}$$

as an eigenvalue problem for Ra in terms of A, P, ν and the spanwise wavenumber, k. The aim then is to minimise Ra with respect to both ν and k. The principle of exchange of stabilities applies to Eqs. (12) and (13) (see Appendix A) and therefore we may set $\omega = 0$. We also mention that the two-dimensional problem which was investigated by Rees and Tyvand [10] is obtained from that defined by Eqs. (12) in the limit $k \to 0$, i.e. when the disturbances become independent of y.

The eigenvalue problem given by Eqs. (12) and Eq. (13) was solved using precisely the same numerical scheme that was devised in Rees and Tyvand [10] and described there in great detail. Briefly, the two ordinary differential equations were approximated using an eighth order finite difference method where the resulting difference equations were rearranged into the form of a matrix eigenvalue problem for Ra. With such a high order method, numerical accuracy of at least six significant figures could be obtained with a relatively small number of grid points. In general we used 40 intervals per unit distance. Accuracy of encoding the method was provided by a comparison with solutions obtained using a fourth order Runge-Kutta scheme coupled with

a shooting method. Neutral curves, some of which will be presented below, generally provided a single minimum. This minimum was found by means of a Newton-Raphson scheme applied to five values of Ra which were obtained for five closely-spaced values of k. Thus, if we write $Ra = Ra(k)$, then we require those values of k for which $dRa/dk = 0$. Thus corrections in k are given by the standard formula,

$$\delta k = -Ra'(k)/Ra''(k), \tag{14}$$

where the following fourth order central difference approximations are used to approximate the above derivatives,

$$Ra'(k) \simeq \left[\tfrac{1}{12}Ra(k-2\epsilon) - \tfrac{2}{3}Ra(k-\epsilon) + \tfrac{2}{3}Ra(k+\epsilon) - \tfrac{1}{12}Ra(k+2\epsilon)\right]/\epsilon, \tag{15a}$$

$$Ra''(k) \simeq \left[-\tfrac{1}{12}Ra(k-2\epsilon) + \tfrac{4}{3}Ra(k-\epsilon)\tfrac{5}{2}Ra(k) + \tfrac{4}{3}Ra(k+\epsilon) - \tfrac{1}{12}Ra(k+2\epsilon)\right]/\epsilon^2. \tag{15b}$$

Minimisation using these approximations yielded at least three if not more than four figures of accuracy even when ϵ is as large as 0.01, which is well in excess of what is required for graphical resolution.

4 Discussion of the results

4.1 Mode shapes

Before we present details of the neutral curves and the minimisation of the critical values of Ra over k and ν, it is important to have an idea about what the computed solutions look like. While the present computations are one-dimensional, the onset modes are three-dimensional, but the mode shapes themselves are visualised easily by plotting contours of the rate of heat transfer at either the upper or lower surfaces of the layer, and this yields a two-dimensional view of how the disturbance varies with x and y.

Figure 2 compares onset modes for the two amplitudes, $A = 0.1$ and $A = 0.3$, for the four cases, $P = 0.5$, $P = 1$, $P = 2$ and $P = 4$. We have selected $k = \pi$ as a representative wavenumbers, and have set $\nu = 0$ so that the onset modes have the same periodicity in the x-direction as the permeability variation. All the plots are confined to the region $0 \le x \le 4$ and $0 \le y \le 2$ for easy comparison, and the values of P are such that the patterns in this Figure tesselate the plane.

When both A and P take small values, then the resulting pattern takes the form of longitudinal rolls at leading order, with small-amplitude variations about this state; this is evident for the case $A = 0.1$ and $P = 0.5$ where the effect of permeability changes is only just visible. As the period increases, then the onset mode becomes increasingly confined to those regions where the permeability takes its largest value. When the amplitude of the permeability variation takes larger

values, then the localisation of the convection pattern becomes more extreme because the local Rayleigh number (i.e. one which is based on permeability at the currently chosen value of x) varies much more greatly over a period. But once the period of the variation is sufficently large, there is little visual difference between the mode shapes for small and large values of A, although larger values of A give profiles which are slightly more concentrated towards the permeability maxima.

Changes in the value of the wavenumber, k, causes the width of the pattern in the y direction to change, as one expects, and therefore it is deemed not necessary to demonstrate this. However, it is an *a priori* expectation that nonzero values of the Floquet exponent could provide the most unstable mode for some choices of A and P. Therefore Figure 3 shows how different values of ν affect the planform of the onset mode. This Figure takes the case $A = 0.3$, $P = 2$ and $k = \pi$, where $0 \leq x \leq 8$ and $0 \leq y \leq 4$, i.e. four periods of the permeability variation and two spanwise periods are displayed.

When $\nu = 0$ we obtain the type of pattern shown in Figure 2 where the longitudinal pattern is still quite evident even though there is much localisation in the regions of high permeability. When $\nu = 1$, regions of positive and negative rates of heat transfer alternate as x increases, and the overall pattern has a period of $2P = 4$ in the x-direction. When $\nu = 0.5$, we show two different forms of the onset mode. The pattern which is labelled, *Oblique*, is the natural pattern which arises due to the substitution which is given in Eq. (11). The line of, say, red spots is aligned at an angle to the x-axis and could be said to form an oblique mode. There is, of course, a second form of this which is equivalent to $\nu = -0.5$, but graphically it may be seen by turning the present plot upside-down. A third form is obtained by adding the two different oblique modes together. This has the effect of removing almost completely any disturbance in alternating regions of high permeability; this is the one labelled as *Rectangular* in Figure 3. The period of each of these three patterns is now $4P = 8$. Other more complcated patterns may be obtained, but these are not shown in the interests of brevity. All of these modes will be referred to below as even modes because the patterns obey the same symmetry as that of the underlying permeability variation.

4.2 Neutral curves

In this subsection we attempt to convey a comprehensive understanding of how the neutral curves vary with the parameters, P, A and ν. While there are only three parameters to vary, this understanding is made more difficult to present than was expected *a priori* because neutral curves corresponding to distinct modes sometimes cross one another. This may be seen in Figure 4 which displays the neutral curves corresponding to various modes for $A = 0.01$ and $A = 0.3$ and for $P = 1$, 1.5, 2, 3, and 4. The value $\nu = 0$ was taken here.

When $k \ll 1$ the first mode to appear is an odd one in x, which means that a dividing (or zero)

disturbance isotherm arises at $x = 0$ and multiples of $x = P$, and therefore a transverse convection cell is centred precisely where the permeability is at its largest. These may be seen in Part 1. The second mode is one for which the temperature field is even in x, as shown in Figures 2 and 3. When either P is sufficiently large or A sufficiently small, the values of Ra for these two modes are almost identical and are indistinguishable graphically. As k increases, the even mode takes over as the one which corresponds to the lower value of Ra. A clear transition of this kind is seen for the case, $A = 0.3$ and $P \leq 2$, which is shown in Figure 4, and it is true for all other cases. For any chosen pair of values of A and P the minimum value of Ra (i.e. the critical Rayleigh number, Ra_c) corresponds to a mode which is even in x in general, and given that k is nonzero, it is also a longitudinal roll. Thus we have already settled the fact that transverse (or two dimensional rolls) never form the most unstable mode.

When $A = 0.01$ the shapes of the neutral curves are seen to depend quite strongly on the period, P. However, the profile of the onset mode can change quite substantially as k increases from zero. If one focusses on the case, $A = 0.01$ and $P = 4$, then the onset mode for very small values of k is roughly proportional to $\sin \pi x$, i.e. it is an odd mode. As k increases, this changes suddenly to the corresonding even mode, $\cos \pi x$, as discussed above. The value of Ra then rises, reaches a maximum and decreases once more. In this region the mode changes gradually to one where the profile has only one minimum and one maximum in the period, P, and although it begins by having both signs, it eventually becomes a single-signed function of x.

Figure 5 concentrates on the neutral curves corresponding to the onset mode, and therefore some curves display a discontinuous change of slope which reflects the crossing of two curves. Here we concentrate on the effect of different values of P on the onset criterion for both $A = 0.1$ and $A = 0.3$, with $k = \pi$ and $\nu = 0$. While it is clear that the critical Rayleigh number is a decreasing function of P, the value of Ra close to $k = 0$ is not a monotonic function of P. This is caused by the difficulty of fitting cells, which would naturally have a wavelength of 2 into the period of the permeability variations. Indeed, Part 1 shows that this is achieved only by selecting nonzero values of ν to allow an appropriate spatial period of the onset profile. When P takes small values, the neutral curve is almost identical to that for the uniform porous layer, and the profile of the onset mode is generally very similar to that given in Figure 2 for $P = 0.5$, i.e. it is a longitudinal vortex with short wavelength ripples.

Figure 6 is concerned with how the amplitude, A affects the onset criterion when $P = 1$ and $P = 3$. The manner in which the shapes of the neutral curves change with A is much more straightforward than how they change with P. The critical value, Ra_c, is a decreasing function of A in general. This is because of the presence of regions of permeability which are higher than the mean value that used to define the Rayleigh number.

The effect of varying ν is shown in Figure 7 for $A = 0.3$, $k = \pi$ and for the two periods, $P = 0.8$ and $P = 2$. When $P = 0.8$ it is clear that the smallest value of Ra_c is obtained when $\nu = 0$, but when $P = 2$ it is $\nu = 1$. In Part 1 it was found that the minimising value of ν for two dimensional convection varies smoothly between $\nu = 0$ and $\nu = 1$ and back. For three dimensional convection we find that the transitions are always sudden, and that they arise for all amplitudes, A. These graphs also suggest that Ra_c varies monotonically with ν, which is actually not true in general. For a chosen value of A, there is a transitional value of P where $\nu = 1$ takes over from $\nu = 0$ as the minimising value. In such cases Ra_c increases from its $\nu = 0$ value to a maximum and then it decreases again towards its $\nu = 1$ value. Thus the transition in terms of ν is always discontinuous.

4.3 Critical values

All of this is summarised in Figure 8 which displays the variation in Ra_c and k_c with P for a wide selection of values of A ranging from 0.01 to 0.9. First of all, we note that this Figure confirms that Ra_c is a decreasing function of both A and P in all cases. Second, Ra_c appears to tend towards $4\pi^2$ when $P \to 0$ independently of the value of A. Third, the region in between the two black circles for each Ra_c curve is the region in which $\nu = 1$ comprises the most unstable mode. There appears only to be one such region; values of P which are outside of this range correspond to $\nu = 0$. The $\nu = 0$ curve, when it doesn't form the most unstable mode, is shown as a dotted line in this graph.

The corresponding wavenumbers are also shown. There is a tendency for $k \to \pi$ as $P \to 0$ and as $P \to \infty$. Somewhat surprisingly the value of k_c is quite small on the $\nu = 1$ side of the first transition when A is small. Such a mode looks more like a transverse roll with a relatively slow modulation in the y-direction but with a wavenumber roughly equal to π in the x-direction. This happens because $P = 1$ together with $\nu = 1$ yields a potential pattern in the x-direction which has a period of 2. Although it is tempting to cite this as a potential reason for having $\nu = 1$ solutions being favoured near to $P = 1$, it doesn't explain why the range of P over which $\nu = 1$ is favoured is so large.

The locus of points where the favoured mode makes its transition between $\nu = 0$ and $\nu = 1$ is shown in Figure 9. The numerical values of P corresponding to the lower branch tend towards 1 as $A \to 0$, and therefore $\nu = 0$ forms the favoured mode whenever $P < 1$ for all amplitudes, A. With regard to the upper branch, the values of P appear to increase without bound as $A \to 0$, and it appears to satisfy a relation which is approximately of the form, $P \sim 1.74A^{-1/4}$. When $A = 0.001$ then $P = 9.5760$ on the upper branch.

5 Conclusions

This paper is a natural extension of the two dimensional analysis of Part 1 into three dimensions. We have considered the effect of spatially periodic variations in the permeability on the onset of convection in an otherwise uniform horizontal porous layer heated from below. When convection is confined to be two dimensional, the critical parameters for the onset of convection were found in Part 1 to depend not only on the period and the amplitude of the permeability variations but also only on the Floquet exponent. For example, the Floquet exponent corresponding to the most unstable mode changes continuously as the period of the variations change. In the present paper it has been shown that, when convection is allowed to be three dimensional, the Floquet exponent only ever changes discontinously as P increases from zero, and it does this only twice, namely from $\nu = 0$ to $\nu = 1$ when P takes a value which is a little greater than 1, and then a second time back to $\nu = 0$ at a value of P which is much more strongly dependent on the value of A. It is also found that the critical Rayleigh number always decreases as either P increases or A increases.

References

[1] C. W. Horton, F. T. Rogers, Convection currents in a porous medium, Journal of Applied Physics 16 (1945) 367–370.

[2] E. R. Lapwood, Convection of a fluid in a porous medium, Proceedings of the Cambridge Philosophical Society 44 (1948) 508–521.

[3] D. A. Nield, A. Bejan, Convection in Porous Media, 4th Edition, Springer-Verlag, New York, 2013.

[4] E. Palm, J. E. Weber, O. Kvernvold, On steady convection in a porous medium, Journal of Fluid Mechanics 54 (1972) 153–161.

[5] R. McKibbin, M. J. O'Sullivan, Onset of convection in a layered porous medium heated from below, Journal of Fluid Mechanics 96 (1980) 375–393.

[6] D. A. S. Rees, D. S. Riley, The three-dimensional stability of finite-amplitude convection in a layered porous medium heated from below, Journal of Fluid Mechanics 211 (1990) 437–461.

[7] D. A. Nield, C. T. Simmons, A discussion on the effect of heterogeneity on the onset of convection in a porous medium, Transport in Porous Media 68 (2007) 413–421.

[8] A. De Wit, G. M. Homsy, Viscous fingering in periodically heterogeneous porous media. I. Formulation and linear instability, The Journal of Chemical Physics 107 (1997) 9609–9618.

[9] A. De Wit, G. M. Homsy, Viscous fingering in periodically heterogeneous porous media. II. Numerical simulations, The Journal of Chemical Physics 107 (1997) 9619–9628.

[10] D. A. S. Rees, P. A. Tyvand, Onset of convection in a porous layer with continuous periodic horizontal stratification. Part I. Two-dimensional convection, Transport in Porous Media 77 (2009) 187–205.

Appendix A – Exchange of stabilities

This analysis proceeds by first multiplying Eq. (12a) by $F\exp(i\lambda\nu x/2)$, and Eq. (12b) by $\exp(i\lambda\nu x/2)$ and rearranging them thus:

$$\Big(Ff'e^{i\lambda\nu x/2}\Big)' + \tfrac{i\lambda\nu}{2}\Big(Ffe^{i\lambda\nu x/2}\Big)' - (k^2+\pi^2)Ffe^{i\lambda\nu x/2} - \pi Fhe^{i\lambda\nu x/2} = 0, \tag{A1a}$$

$$\Big(h'e^{i\lambda\nu x/2}\Big)' + \tfrac{i\lambda\nu}{2}\Big(he^{i\lambda\nu x/2}\Big)' - (k^2+\pi^2-i\omega)he^{i\lambda\nu x/2} + Ra\,F(h+\pi f)e^{i\lambda\nu x/2} = 0. \tag{A1b}$$

These equations are now multiplied by the functions, $\bar{f}\exp(-i\lambda\nu x/2)$ and $\bar{h}\exp(-i\lambda\nu x/2)$, respectively, and integrated over one period, P. This is a legitimate step to take because the integrands of both integrals have precisely this period. The resulting equations may be added together in such a way that an integral involving $Fh\bar{f}$ is removed, and we thereby obtain,

$$\begin{aligned} i\omega\int_0^P |h|^2\,dx \;&= \int_0^P \Big[|h'|^2 + \Big(k^2+\pi^2+\tfrac{1}{4}\lambda^2\nu^2 - Ra\,F\Big)|h|^2 + \tfrac{i\lambda\nu}{2}\Big(h\bar{h}' - h'\bar{h}\Big)\Big]\,dx \\ &\quad + Ra\int_0^P F\Big[|f'|^2 + \Big(k^2+\pi^2+\tfrac{1}{4}\lambda^2\nu^2\Big)|f|^2 + \tfrac{i\lambda\nu}{2}\Big(f\bar{f}' - f'\bar{f}\Big)\Big]\,dx. \end{aligned} \tag{A2}$$

All the terms on the right hand side of this equation are real, while the left hand side is purely imaginary. Therefore this equation may be satisfied if and only if $\omega = 0$. We therefore conclude that the principle of exchange of stabilities holds for all values of the given parameters, and that the onset problem is stationary.

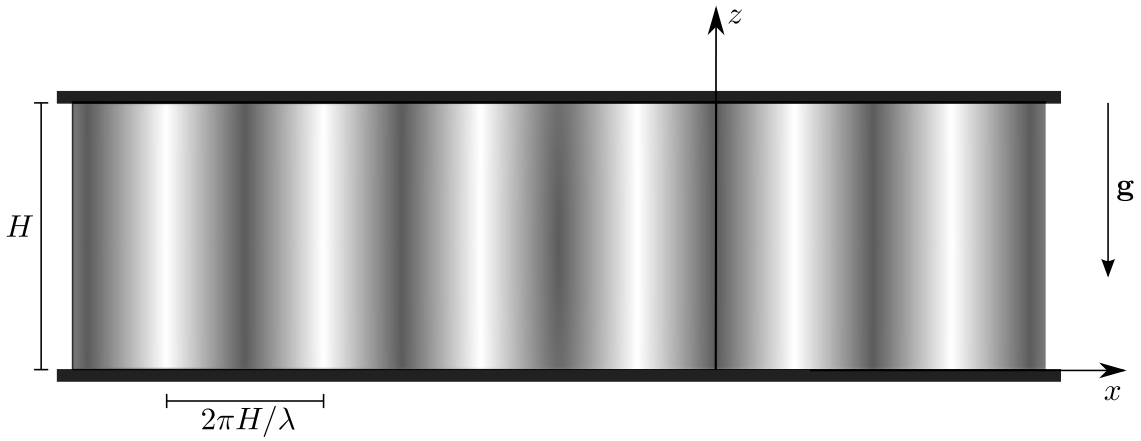

Figure 1: The fluid-saturated porous layer with a periodic horizontal permeability field.

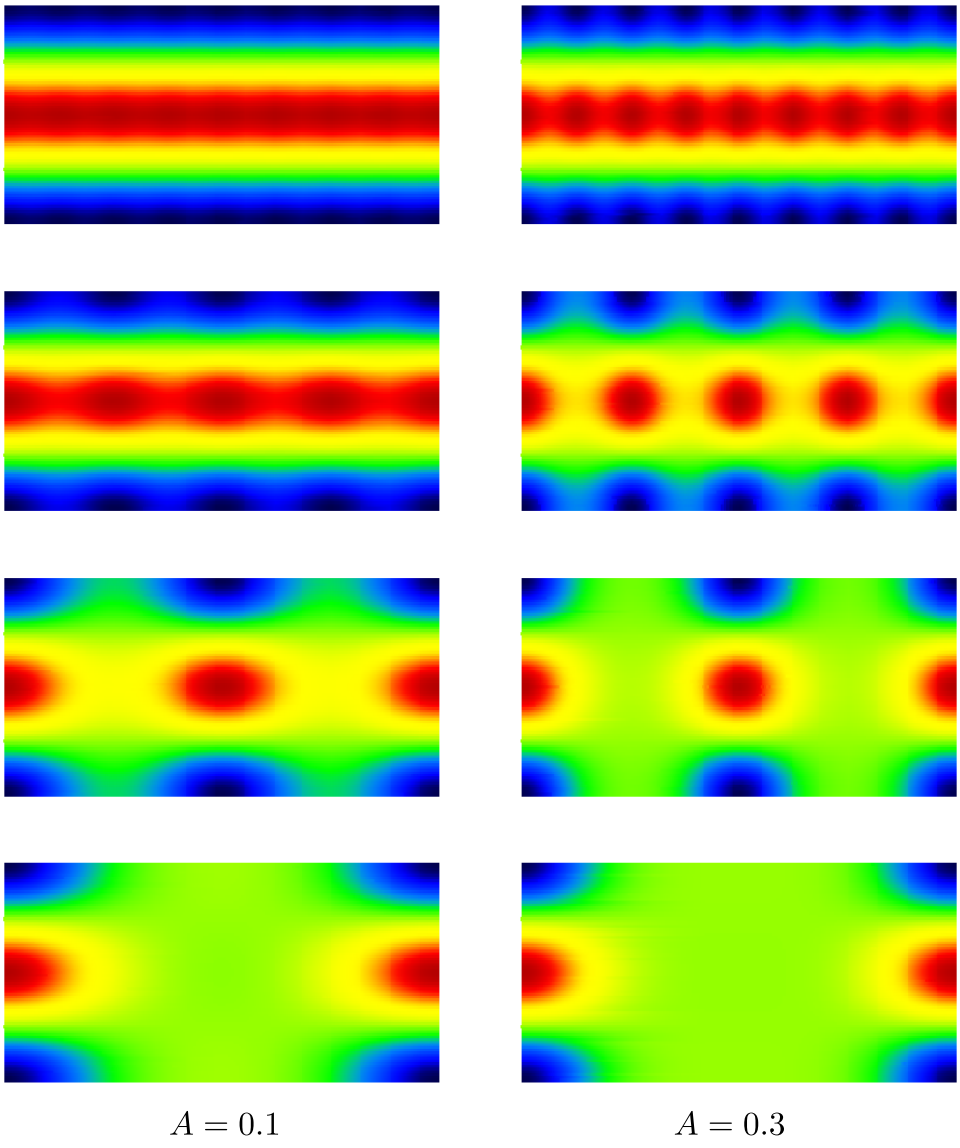

Figure 2: Showing the lower surface rate of heat transfer for different onset modes for $A = 0.1$ (left) and $A = 0.3$ (right), and for $P = 0.5$ (uppermost), 1, 2 and 4 (lowest). Here $k = \pi$ and $\nu = 0$ and the shown patterns are confined to $0 \leq x \leq 4$ and $0 \leq y \leq 2$.

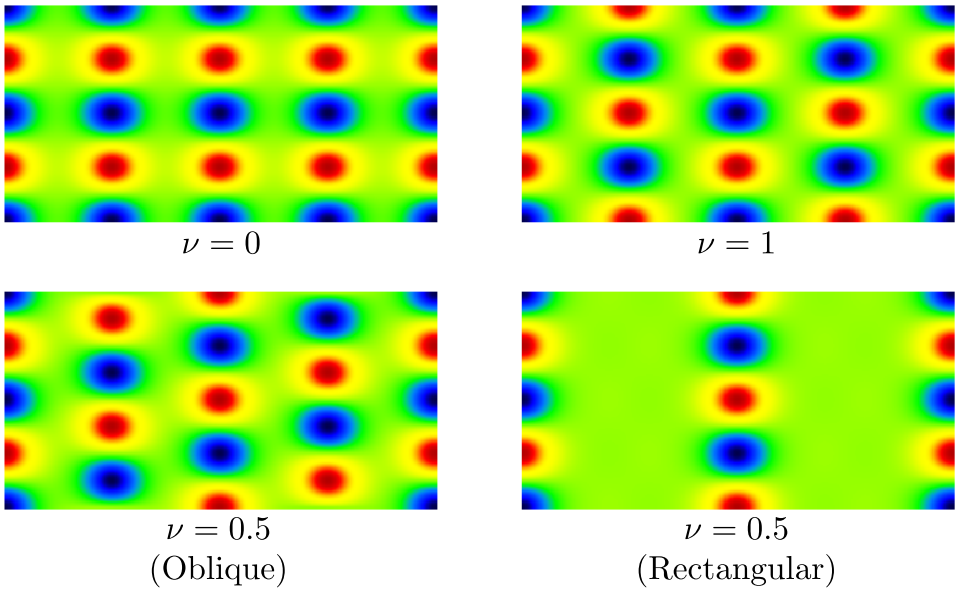

Figure 3: Showing the lower surface rate of heat transfer for different onset modes for the case, $P = 2$, $A = 0.3$ and $k = \pi$, and for the values of ν shown.

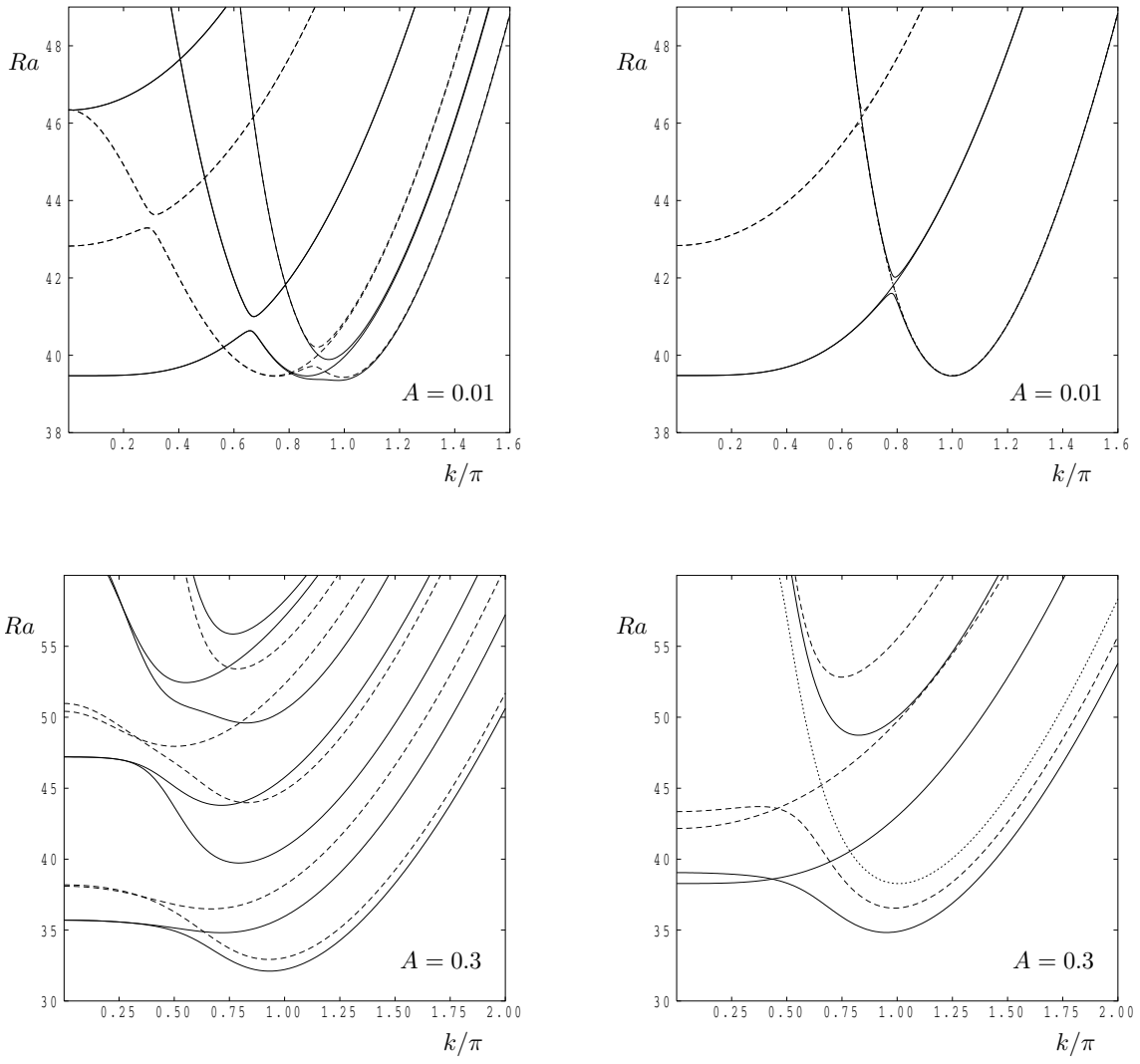

Figure 4: Showing how neutral curves vary with P for $A = 0.1$ and $A = 0.3$. Here $k = \pi$ and $\nu = 0$. In the two left hand frames continuous lines depict $P = 4$ and dashed lines $P = 3$. In the right hand frames continuous lines depict $P = 2$, dashed lines $P = 1.5$ and dotted lines $P = 1$. Up to six modes are displayed.

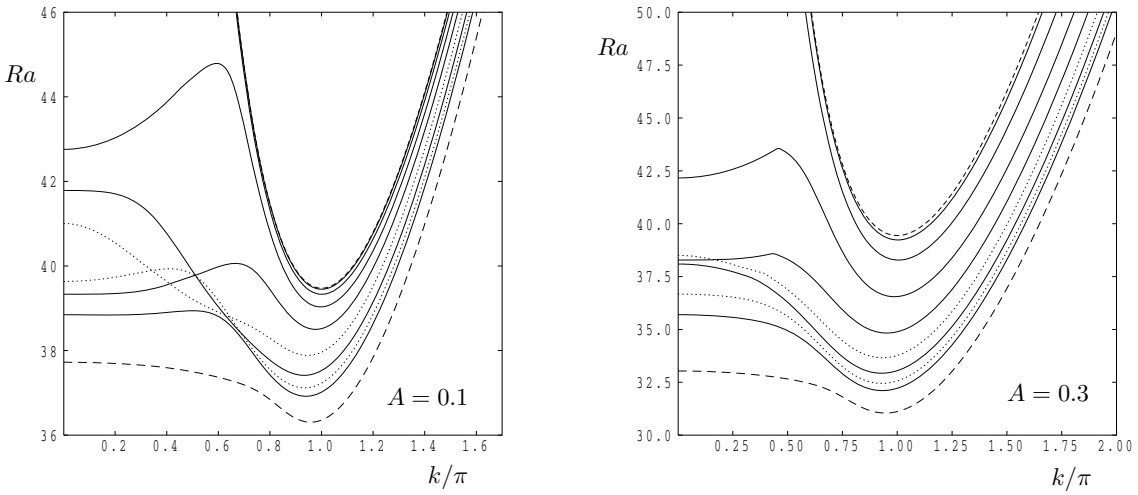

Figure 5: Showing the neutral curves corresponding to the first mode for $P = 0.2$ (short dashes), 0.5, 1, 1.5, 2, 2.5, 3, 3.5, 4 and 8 (long dashes). Curves corresponding to $P = 2.5$ and 3.5 are dotted. Here $A = 0.1$ (left frame) and $A = 0.3$ (right frame) with $k = \pi$ and $\nu = 0$.

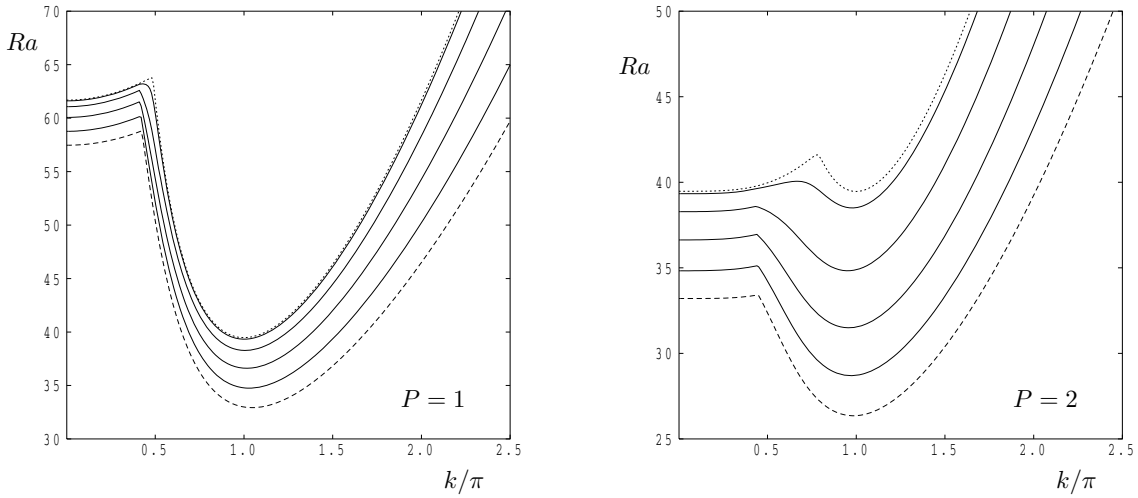

Figure 6: Showing the neutral curves corresponding to the first mode for $A = 0.01$ (short dashes), 0.1, 0.3, 0.5, 0.7 and 0.9 (long dashes). Here $P = 1$ (left frame) and $P = 2$ (right frame) with $k = \pi$ and $\nu = 0$.

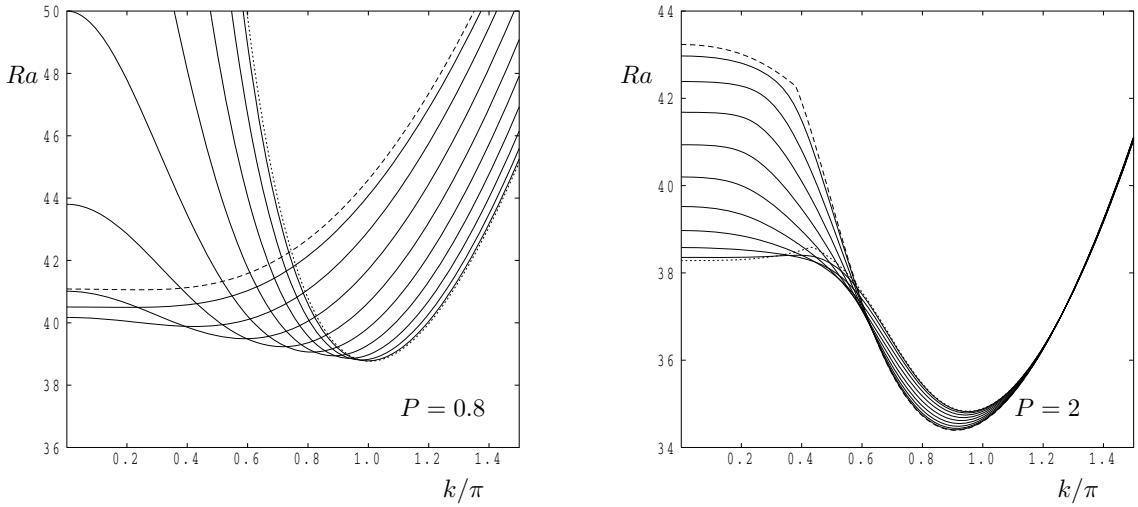

Figure 7: Showing variation with ν of the neutral curves corresponding to the first mode for $A = 0.3$ and $k = \pi$. The left frame corresponds to $P = 0.8$ and the right to $P = 2$. Dotted lines correspond to $\nu = 0$ and dashed lines to $\nu = 1$. The values of ν are separated by an increment of 0.1.

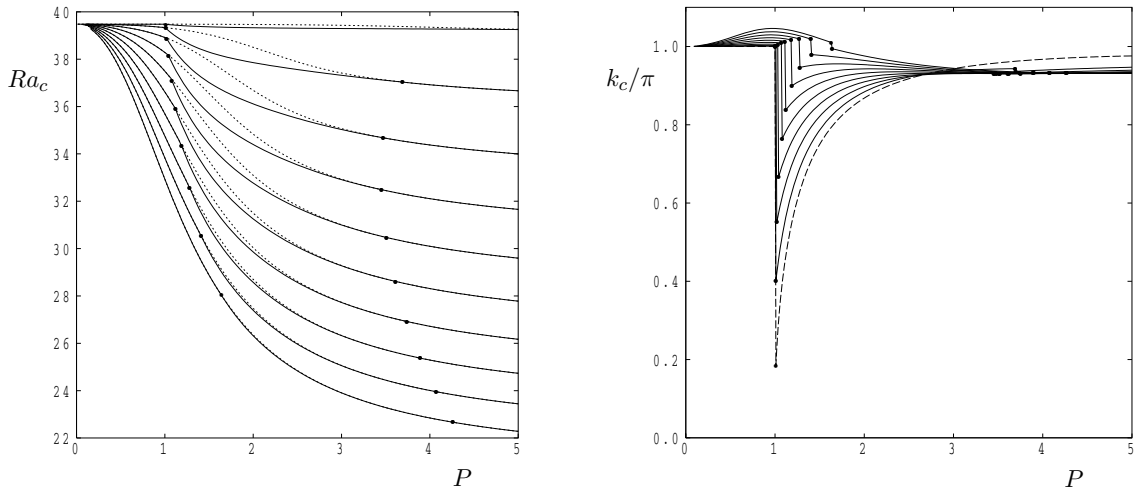

Figure 8: Showing the variation of the critical values of Ra_c (left) and k_c (right) with P for $A = 0.01$, 0.1, 0.2, 0.3 (0.1) 0.9. For each Ra_c curve the two filled circles delineate the range of P over which $\nu = 1$ yields the smallest value of Ra_c, while $\nu = 0$ elsewhere. For Ra_c the uppermost line corresponds to $A = 0.01$; for k_c it is the dashed line.

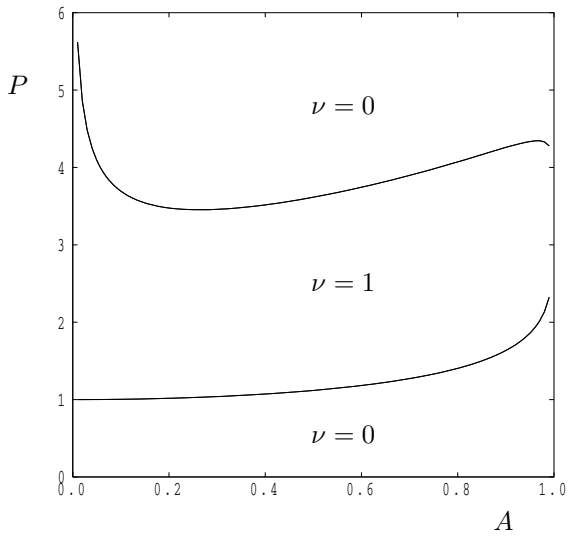

Figure 9: Showing the regions in (A, P)–space in which either $\nu = 0$ or $\nu = 1$ forms the favoured onset mode.